


Article

Electrical Method for In Vivo Testing of Exhalation Sensors Based on Natural Clinoptilolite

Gianfranco Carotenuto ^{1,*}  and Luigi Nicolais ²

¹ Institute for Polymers, Composites and Biomaterials (IPCB-CNR), National Research Council, Piazzale E. Fermi, 80055 Naples, Italy

² Engineering Faculty, University of Naples “Federico II”, Corso Nicolangelo Protopisani, 80146 Naples, Italy; nicolais@unina.it

* Correspondence: giancaro@unina.it; Tel.: +39-3384045292

Abstract: Natural substances with a complex chemical structure can be advantageously used for functional applications. Such functional materials can be found both in the mineral and biological worlds. Owing to the presence of ionic charge carriers (i.e., extra-framework cations) in their crystal lattice, whose mobility is strictly depending on parameters of the external environment (e.g., temperature, humidity, presence of small gaseous polar molecules, etc.), zeolites can be industrially exploited as a novel functional material class with great potentialities in sensors and electric/electronic field. For fast-responding chemical-sensing applications, ionic transport at the zeolite surface is much more useful than bulk-transport, since molecular transport in the channel network takes place by a very slow diffusion mechanism. The environmental dependence of electrical conductivity of common natural zeolites characterized by an aluminous nature (e.g., chabasite, clinoptilolite, etc.) can be conveniently exploited to fabricate impedimetric water-vapor sensors for apnea syndrome monitoring. The high mechanical, thermal, and chemical stability of geomorphic clinoptilolite (the most widely spread natural zeolite type) makes this type of zeolite the most adequate mineral substance to fabricate self-supporting impedimetric water-vapor sensors. In the development of devices for medical monitoring (e.g., apnea-syndrome monitors), it is very important to combine these inexpensive nature-made sensors with a low-weight simplified electronic circuitry that can be easily integrated in wearable items (e.g., garments, wristwatch, etc.). Very low power square-wave voltage sources (micro-Watt voltage sources) show significant voltage drops under only a minimal electric load, and this property of the ac generator can be advantageously exploited for detecting the small impedimetric change observed in clinoptilolite sensors during their exposition to water vapor coming from the human respiratory exhalation. Owing to the ionic conduction mechanism (single-charge carrier) characterizing the zeolite slab surface, the sensor biasing by an ac signal is strictly required. Cheap handheld multimeters frequently include a very low power square-wave (or sinusoidal) voltage source of different frequency (typically 50 Hz or 1 kHz) that is used as a signal injector (signal tracer) to test audio amplifiers (low-frequency amplifiers), tone control (equalizer), radios, etc. Such multimeter outputs can be connected in parallel with a true-RMS (Root-Mean-Square) ac voltmeter to detect the response of the clinoptilolite-based impedimetric sensors as voltage drop. The frequency of exhalation during breathing can be measured, and the exhalation behavior can be visualized, too, by using the voltmeter readings. Many handheld multimeters also include a data-logging possibility, which is extremely useful to record the voltage reading over time, thus giving a time-resolved voltage measurement that contains all information concerning the breathing test. Based on the same principle (i.e., voltage drop under minimal resistive load) a devoted electronic circuitry can also be made.

Keywords: clinoptilolite; impedimetric sensor; surface conductivity; apnea syndrome monitoring; voltage drop



Citation: Carotenuto, G.; Nicolais, L. Electrical Method for In Vivo Testing of Exhalation Sensors Based on Natural Clinoptilolite. *Coatings* **2022**, *12*, 377. <https://doi.org/10.3390/coatings12030377>

Academic Editor: María Dolores Fernández Ramos

Received: 21 February 2022

Accepted: 10 March 2022

Published: 13 March 2022

Publisher's Note: MDPI stays neutral with regard to jurisdictional claims in published maps and institutional affiliations.



Copyright: © 2022 by the authors. Licensee MDPI, Basel, Switzerland. This article is an open access article distributed under the terms and conditions of the Creative Commons Attribution (CC BY) license (<https://creativecommons.org/licenses/by/4.0/>).

1. Introduction

Materials with a unique combination of properties (multifunctional materials) can be found among natural substances characterized by significant structural complexity [1]. When a possible application for such nature-made materials has been identified, the development of a device with performance comparable to that of systems based on artificial substances can follow [2]. There are also examples in the literature in which similar technological results cannot be reached with comparable performance by using manmade materials [3,4]. As a consequence, the capability to identify the applicative potentiality hidden in the most common natural substances represents the key factor to come in the technological exploitation of nature-made materials, thus promoting sustainability. Among the different available natural substances, the most powerful potentialities have been found in complex types of solids, since their artificial replication is quite difficult [5,6]. Numerous natural systems have extreme complexity, because complexity is the intrinsic characteristic of the whole natural world [7]. For example, there are a number of biological tissues, mineral substances, and biominerals with specific physical properties, such as piezoelectricity, electrical conductivity, magnetism, etc. (e.g., onion skin, diatomite, eggshell, etc.) [1,2], that are advantageously exploitable for different technological applications.

Natural zeolites represent an interesting class of multifunctional materials, and a number of potentially useful physical and chemical characteristics of these mineral substances have been industrially exploited [8–14]. Usually, natural zeolites have a quite low Si/Al atomic ratio, and for such a reason they are named “aluminous zeolites”, in contrast with the “high-siliceous zeolites” that are mainly originated by synthesis. Owing to the aluminum atoms contained in these chemical compounds, the presence of as many extra-lattice cations required to balance the negative charge localized on the aluminum atom follows. Natural zeolites contain different types of cations (typically Na^+ , K^+ , Ca^{2+} , Mg^{2+} , and Fe^{3+}), and since these cations may have single or multiple charge, there is a significant fraction of the aluminum atoms in the lattice with unbalanced negative charge. Consequently, electrical transport in zeolite lattice becomes possible by cation hopping among the neighbor negatively charged sites [15,16]. Natural zeolites are therefore solid-state ionic conductors with single-charge carrier (usually corresponding to the largest monovalent cations present in crystal lattice, since they have the lowest charge density [17]). However, these crystalline solids may conduct electricity only at high temperature (since in this case a larger fraction of charge carriers have enough energy exceeding the activation barrier required for jumping between the nearest negative sites) or by hydration/solvation (because in this case the Coulomb interaction between cations and the negative sites decreases) [18–21]. Owing to the presence of a regular array of few angstrom-sized channels (1–13 Å) crossing the zeolite crystal lattice, all cations in the lattice can be solvated only by small polar molecules, that is, molecules with an average size lower than the channel diameter; these include, for example, molecules of water, methanol, formaldehyde, etc. Consequently, natural zeolite crystals can be technologically exploited as both thermal and chemical sensors [22]. In their use as chemical sensor, these materials are able to promptly modify their external surface electrical conductivity by exposition to water vapor. The surface electrical conductivity of natural zeolites with Si/Al close to 5 (e.g., clinoptilolite) may change significantly by exposition to water vapor, and in addition the water molecules spontaneously desorb from these slightly hydrophobic materials when these last are removed from the humid environment. Therefore, zeolite chemical sensors show completely reversible electrical behavior with fast return to the original electrical conductivity value. Owing to the involved ionic conduction mechanism, impedance measurements are required for zeolitic sensors. Sinusoidal or square-wave signals with frequency lower than 1 kHz can be conveniently used. A slab of natural zeolite with a convenient value of the Si/Al ratio can be used as a gas-phase water sensor, and, according to the literature [23], geomorphic clinoptilolite has shown to be very adequate for such an application.

Natural clinoptilolite is the most widely spread zeolite type of natural origin [24]. This crystalline substance is characterized by low cost and excellent mechanical, ther-

mal, and chemical resistance. A slab of natural clinoptilolite has a polycrystalline nature made of highly compacted few micron-sized single lamellar crystals [25,26]. Geomorphic clinoptilolite can be readily used to fabricate water-vapor sensors by applying two parallel electrodes to the surface of a small and perfectly flat slab. The electrodes can be simply obtained by painting two very close rectangular areas on the slab surface by using silver paint. Electrodes must be located on the slab surface in order to exclude from the electrical transport mechanism those cations belonging to internal channel surface. Thus, preventing the slow diffusive mass transport mechanism involved in the solvation of inner cations, the maximum response-fastness possible for this ceramic sensor can be achieved. Owing to the excellent mechanical resistance of clinoptilolite, very robust self-supporting sensors can be fabricated. For the high thermal stability of clinoptilolite, these water-vapor sensors can be exploited for technological applications also at temperatures higher than room temperature.

Recently, the use of naturally available nanostructured mineral substances (e.g., halloysite nanotubes, sepiolite nanofibers, attapulgite, etc.) in the fabrication of resistive humidity sensors to be used for different body-related-humidity-detection applications (e.g., respiratory behavior, speech recognition, skin moisture, non-contact switch, diaper monitoring, etc. [27]) has been proposed in the literature [28–30]. These nature-made sensitive materials have shown good humidity-sensing performances at different relative humidity (RH) conditions, and, in addition, their use represents a facile, low-cost, and environmentally friendly strategy to achieve high-performance sensing devices, without requiring complex manufacturing approaches frequently adopted in this field [31–33].

Inexpensive fast-response ceramic moisture sensors can be conveniently used as devices for apnea syndrome control (i.e., human exhalation sensors) [34–36] by using a miniaturized wearable electric revelation technique. Here, the capability of geomorphic clinoptilolite sensor to promptly and reversibly detect the humidity exhaled during breathing was evaluated by using the “voltage-drop” technique, an original instrumental approach that requires very simple electronic circuitry. Device miniaturizing needs extremely reduced electronic circuitry, which is essential for the wearability of these health monitors (e.g., apnea-syndrome monitor).

2. Materials and Methods

A commercial sample of natural clinoptilolite (TIP—Technische Industrie Produkte, GmbH, Waibstadt, Germany) was used in the as-received form for fabricating prototypes of the impedimetric sensor. In particular, the sensors were obtained by cutting the raw zeolite piece in the form of rectangular slabs of small thickness (5.0 mm × 10.0 mm × 3.0 mm) by using a mini electric cutting machine (electric mini-grinder, VUM-40, Vigor, Fossano (CN), Italy, equipped with a diamond cutting wheel). Two electrical contacts (1 mm spaced) were painted on the slab surface by using a curable silver paste (EN-06B8, ENSON, Shenzhen, China), and wires were cold-welded to the electrodes by the same paint. According to silver-paste specifications, the obtained device was left to dry in air for 2 days and then baked in an oven at 140 °C for 30 min. Two-lead measurements were used to test the moisture sensor; this type of measurement involves a small contact resistance due to the silver–zeolite interface that slightly reduces the device sensitivity. Since the silver electrodes are located at the zeolite surface, only hydrated monovalent cations (i.e., KOH^{2+}) belonging to external surface can participate in the electrical transport.

The clinoptilolite sample morphology was investigated by scanning electron microscopy (SEM, Quanta 200 FEG microscope, FEI, Hillsboro, OR, USA) after its powdering by a hammer. The characteristic Si/Al molar ratio and the type of extra-framework cations present in the mineral were determined by using energy-dispersive X-ray spectroscopy (EDS, Inca 250, Oxford Instruments, Oxford, UK). The type of crystalline solid phases present inside the mineral were identified by using large-angle powder diffraction (XRD, X'Pert PRO, PANalytical, Oxford, UK).

A handheld digital multimeter (DMM, UT-71D, Uni-Trend, Dongguan, China) was used as a true-RMS voltmeter for measuring the voltage across the ac generator output,

when it was connected in parallel to the zeolite-based humidity sensor. The DMM included an optically insulated high-speed data-logging system, which allowed the multimeter to record voltage measurements at a speed of 8–9 Sa/s (sampling per second). Such high-speed voltage recording required setting the multimeter in low-resolution mode (4000 counts). In particular, DMM was connected to a PC by a cable, and measurements were recorded by using a dedicated software (UTC/D/E Interface Program, version 3.00, 2017, Uni-Trend Technology, Dongguan, China). Square-wave voltage sources embedded into different handheld DMMs (i.e., DT830D, DT-830B, DT832, ANENG AN8206, ANENG AN8008, KONIG KDM-100, and UT20B) were tested. The best results, in terms of lowest power source, were found with the square-wave source embedded in the DT830D digital multimeter (cheap entry-level DMM, available under different trademarks). The square-wave trace was obtained by an analog oscilloscope (AO-610-2 10 MHz, Voltcraft, distributed by Conrad Electronic SE, Hirschau, Germany), and the harmonic composition of the square-wave signal was obtained by a Fast Fourier Transform (FFT) analysis based on a 2-channel 10 MHz USB oscilloscope (PicoScope 2204A-D2, Pico Technology, Cambridgeshire, UK). A resistance decade box (3280, PeakTech GmbH, Ahrensburg, Germany) was also used to determine the I–V characteristics of the square-wave sources.

3. Results and Discussion

Natural clinoptilolite usually consists of a combination of different crystalline solid phases (zeolites, quartz, etc.), and the clinoptilolite phase is only the principal component of such a natural composite. As a consequence, the exact composition of the mineral needs to be experimentally determined by using the X-ray diffraction technique (XRD). According to the diffractogram shown in Figure 1, the clinoptilolite sample contained the following main crystalline solid phases: clinoptilolite (48.4 wt.%), anorthite (42.0 wt.%), quartz (8.9 wt.%), and stilbite (0.7 wt.%); indeed, the most intensive peaks belonging to the diffraction patterns of these minerals can be clearly detected in the XRD of Figure 1. According to the literature, the found crystalline phase composition is quite typical for clinoptilolite of natural origin [24].

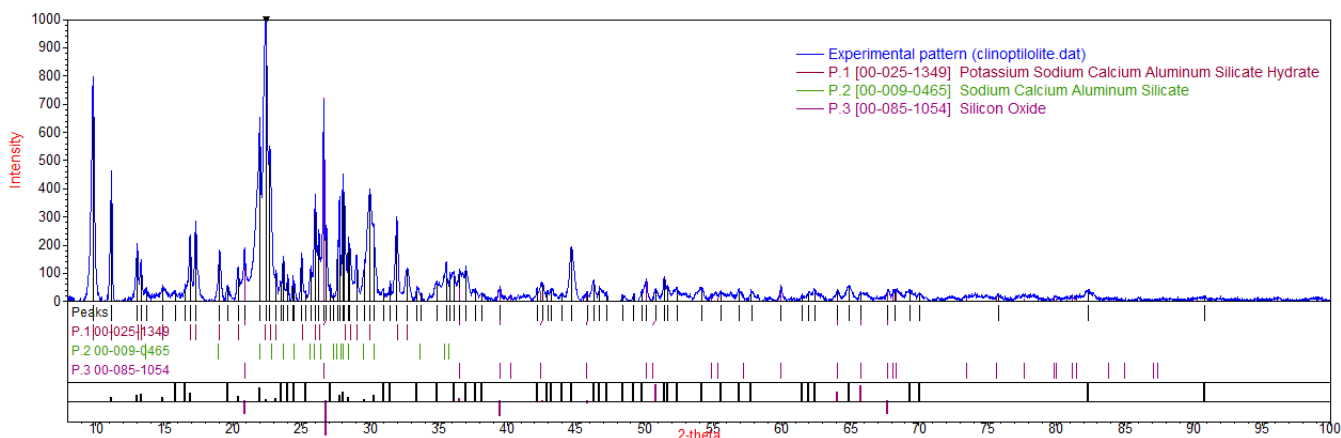


Figure 1. XRD of the natural zeolite used for fabricating the impedimetric water sensor with indication of peaks of the clinoptilolite crystalline phase.

Geomorphic clinoptilolite has a polycrystalline structure. Owing to the extremely high pressure applied to the stone for millions of years, such polycrystalline structure results highly consolidated and characterized by a density (2.15 g/cm^3) close to that of a zeolite single-crystal (absence of macro-porosity) [26]. The clinoptilolite phase is made of perfectly stacked single-lamellar crystals whose morphology can be easily visualized by Scanning Electron Microscopy (SEM) after having delaminated the mineral by applying a strong compressive stress (e.g., hammer blow). The lamellar morphology of the clinoptilolite single crystals is shown in Figure 2a. As visible, all single-lamellar crystals have exactly the

same thickness, corresponding to 40 nm; while the other two sizes range between 300 nm and 1 μm .

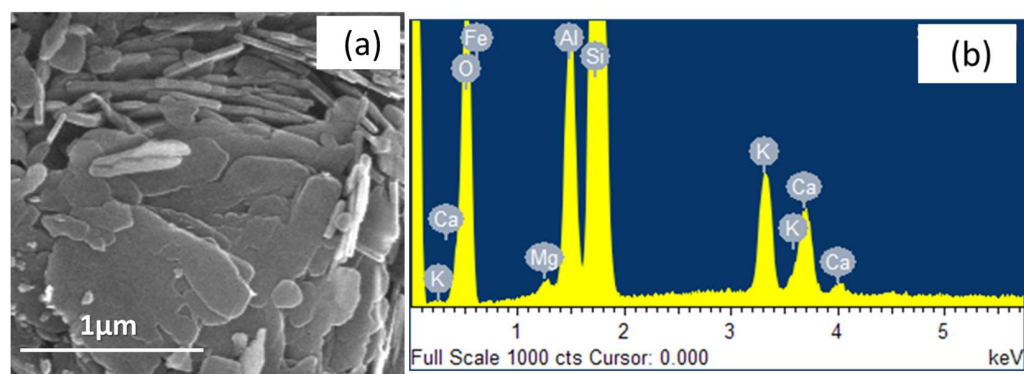


Figure 2. SEM-micrograph of the clinoptilolite single lamellar crystals generated by sample delamination (a) and EDS spectrum of the geomorphic clinoptilolite surface (b).

The characteristic Si/Al molar ratio and the type of extra-framework cations contained in the sample have been established by Energy-Dispersive Spectroscopy (EDS). The EDS-spectrum of the sample is shown in Figure 2b; the specimen contained the following types of cations: K^+ , Ca^{2+} , Mg^{2+} , and Fe^{3+} (in a very little amount). Owing to the low charge density, potassium cations (K^+) were the only charge-carriers active in the transport for this ionic conductor. The Si/Al atomic ratio of the clinoptilolite sample can be approximately evaluated by using the silicon and aluminum intensities of signals in the EDS spectrum, and it corresponded to ca. 5.4. Such a value is typical for this kind of mineral. According to this moderately high Si/Al value, the clinoptilolite sample can be considered as a quite hydrophobic zeolite type. The scarce hydrophilicity of the mineral is a property of fundamental importance for a moisture-sensing material, since it allows the sensor to behave reversibly in service.

Since voltage is an electrical property that is easy to measure, the possibility to use a root-mean-square (RMS) digital voltmeter to detect the wearable sensor response is very convenient. Usually, the response to stimuli of an impedimetric sensor is detected as impedance (Z) variation that is measured by an LCR-meter, or as variation of the intensity of current flowing in the device. However, if the impedimetric sensor is biased by a very low power generator, the sensor response can be detected also as voltage drop at sensor electrodes. In particular, the lower the generator power is, the higher the sensitivity of this method. In addition, the I–V characteristics of the generator can be determined and the voltage response can be converted to current intensity or impedance variation by using the generator I–V characteristics.

Owing to the prompt response and reversible behavior, the moisture sensor based on clinoptilolite can be used as apnea syndrome monitor. The human exhalation pattern could be obtained by measuring the current intensity flowing at sample surface after biasing this sensor, for example, with a 5 kHz sinusoidal voltage signal (20 V_{pp}). However, a similar pattern with much higher resolution can be generated by using the here proposed “voltage-drop” method. To the best of our knowledge, such an instrumental approach, based on a combination of an extremely low power ac generator and true-RMS digital voltmeter, has never been proposed to detect the response of an impedimetric ceramic sensor, such as, for example, a geomorphic zeolite moisture sensor.

When a zeolitic sensor is biased by a sinusoidal or square-wave voltage signal, produced by a standard ac source (function generator with power >1 W), the very high impedance (few $\text{M}\Omega$) of the zeolitic sensor can cause just a negligible voltage drop during the exhalation detection by the sensor. However, many digital multimeters (DMMs) incorporate a square-wave source (signal tracer) of very low power (of the μW order), and if these generators are used to bias the sensor, a significant voltage drop can be experienced

even for a slight variation of the high load impedance. Such a type of signal generator is adequate to detect stimuli by an impedimetric zeolitic sensor by measuring the voltage drop at the sensor electrodes. An alternated voltage source is required to avoid ion accumulation at electrodes surface. In particular, the square-wave output incorporated in the DT830D multimeter originates from the liquid crystal display (LCD) driver in the 7106 multimeter chip. The integrated 7106 is an analog-to-digital converter (ADC), which also provides the LCD back panel driving signal with flipping polarity.

The zeolite sensor was connected to the square-wave output, and a true-RMS digital voltmeter (UT71D digital multimeter, UNI-Trend Technology, Dongguan, China) was placed in parallel to this generator, according to the electrical scheme shown in Figure 3. The square-wave signal characteristics are shown in Figure 4a,b. As visible in the oscilloscope trace, when a coupling capacitor of 10 nF was used to filter the small offset voltage contained in the signal, the power source gave a perfectly symmetrical square-wave with an amplitude of 5.0 V_{pp} (for a square-wave signal, the effective voltage, V_{eff}, as measured by a true-RMS digital voltmeter, exactly corresponds to the peak voltage value, V_p = 2.5). As is visible in Figure 4b, the square-wave signal analysis in the frequency domain showed that the signal was composed by the fundamental at the frequency of 50 Hz and three main odd harmonics.

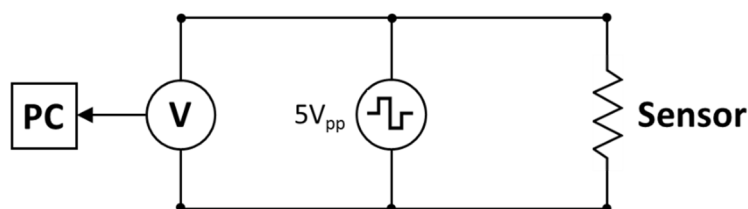


Figure 3. Electrical circuit used to record the voltage-drop measurements.

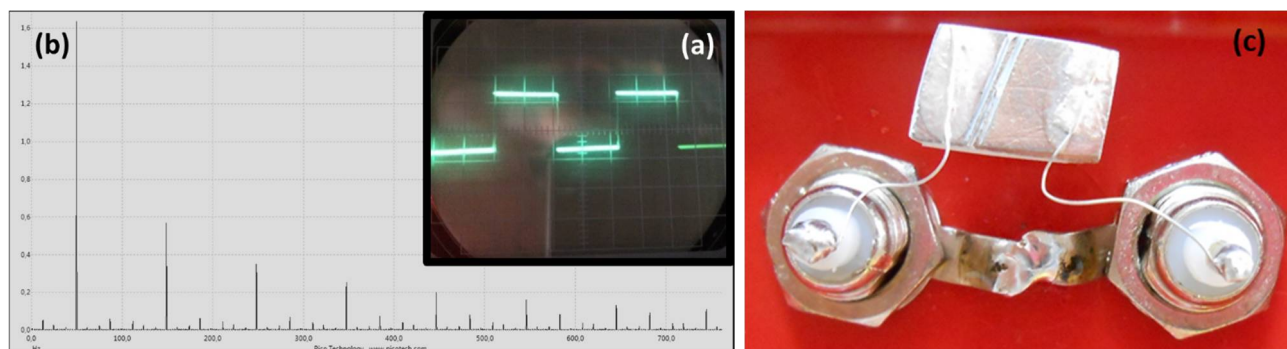


Figure 4. Square-wave signal (a) with its harmonic analysis by FFT oscilloscope (b) and sensor prototype (c).

Time-resolved true-RMS voltage measurements were recorded during exposition to human breathing by using the digital voltmeter UT71D data-logging system. An example of a breathing pattern, including three exhalation steps obtained by the voltage drop technique, is shown in Figure 5. According to this breathing pattern, the surface resistivity was quickly modified in the presence of the water vapor, and the voltage decreased by ca. 100 mV in average. As is visible, water adsorption was a very fast process, and it was described by a linear temporal behavior, while water desorption was slightly slower and followed a parabolic law.

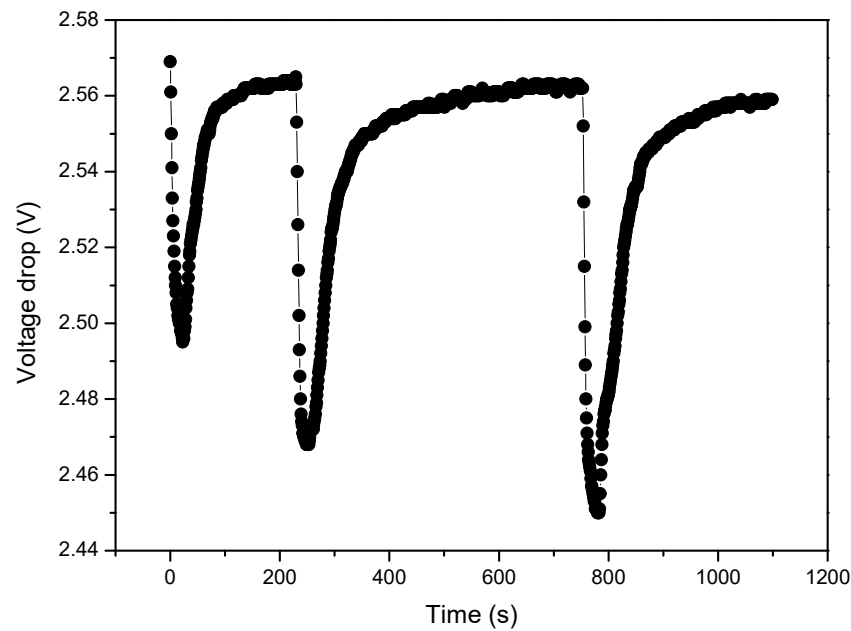


Figure 5. Human-breathing pattern (exhalations) obtained by the voltage drop technique.

The I–V characteristics of the square-wave voltage source are shown in Figure 6a. This curve was obtained by applying to the generator a gradually increasing pure resistive load of a precisely known value (tolerance of resistors: $\pm 1\%$), and measuring the output voltage and the absorbed current by true-RMS digital voltmeter and digital ammeter, respectively. The generator I–V characteristics clearly show a non-ideal behavior, with an electromotive force (EMF) of ca. 2.57 V and an internal resistance value (ratio between the EMF and I_{\max}) of ca. 120 k Ω . In particular, the short-circuit voltage ($V = 0$ and $I = I_{\max}$) and the open-circuit voltage, that is, the voltage without load ($V = V_{\max}$ and $I = 0$), were obtained by extrapolation, since direct measurement of the short-circuit voltage could damage the generator because of the high current intensity flowing in the circuit (overload protection is not present in such simple type of generators), while the open-circuit voltage is limited by the digital multimeter input impedance (usually 10 M Ω at a frequency of 50–60 Hz). In order to avoid the influence of the digital voltmeter input impedance, the voltage and current values were measured for resistive loads inferior to 10 M Ω . As is visible in Figure 6b, the power curve of the square-wave generator shows a dependence of the output power on the applied resistive load, with a maximum value of ca. 14 μ W. Such maximum power is achieved with a pure resistive load of 120 k Ω that corresponds exactly to the internal resistance of the generator.

As indicated above, the exhalation pattern displayed as a voltage-drop sequence (see Figure 5) can be converted to a true-RMS current intensity variation or to a normalized impedance variation by using the determined I–V characteristics of the square-wave generator (see Figure 7a,b). In particular, the following relationship was used to convert the time-resolved voltage-drop measurements to time-resolved current-intensity data:

$$I = I_{sc} \cdot \left(1 - \frac{V}{E}\right), \quad (1)$$

where $I_{sc} = I_{\max} = 21.3 \mu\text{A}$ is the short-circuit current intensity, and E is the electromotive force. Similarly, time-resolved zeolite-sensor impedance (Z) values can be obtained from the experimental voltage data by the following relationship:

$$Z = \frac{V}{I} = \frac{V}{I_{sc} \cdot \left(1 - \frac{V}{E}\right)} = \frac{V}{\left(I_{sc} - \frac{1}{E} \cdot V\right)}, \quad (2)$$

where $r = 120 \text{ k}\Omega$ is the generator internal resistance. As visible, when the breath pattern is expressed as temporal variation of the impedance, the exhalation signals result in being quite deformed (see Figure 7b).

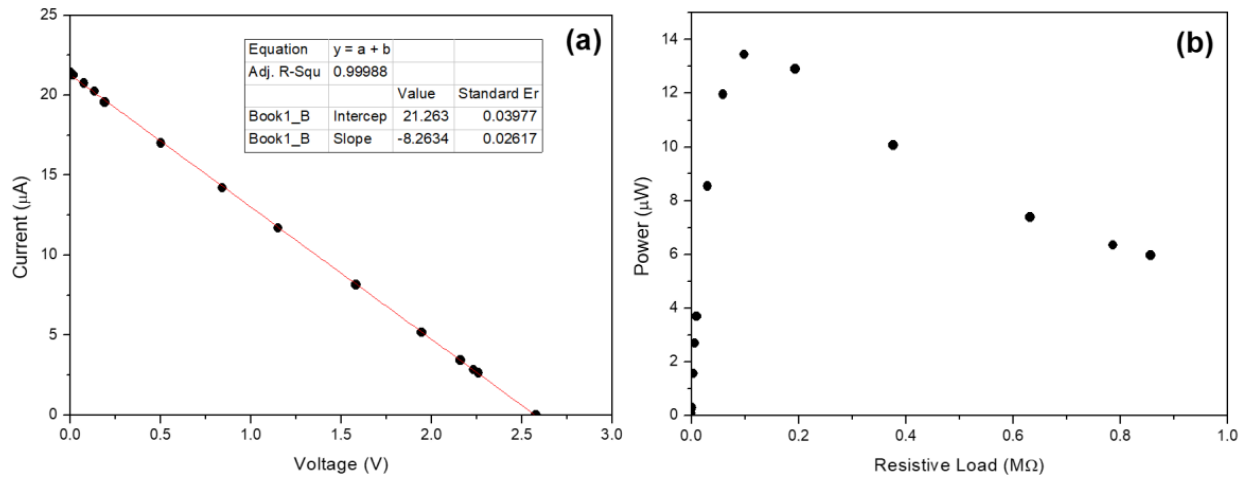


Figure 6. I-V characteristics of the square-wave voltage source (a) and its corresponding power curve (b).

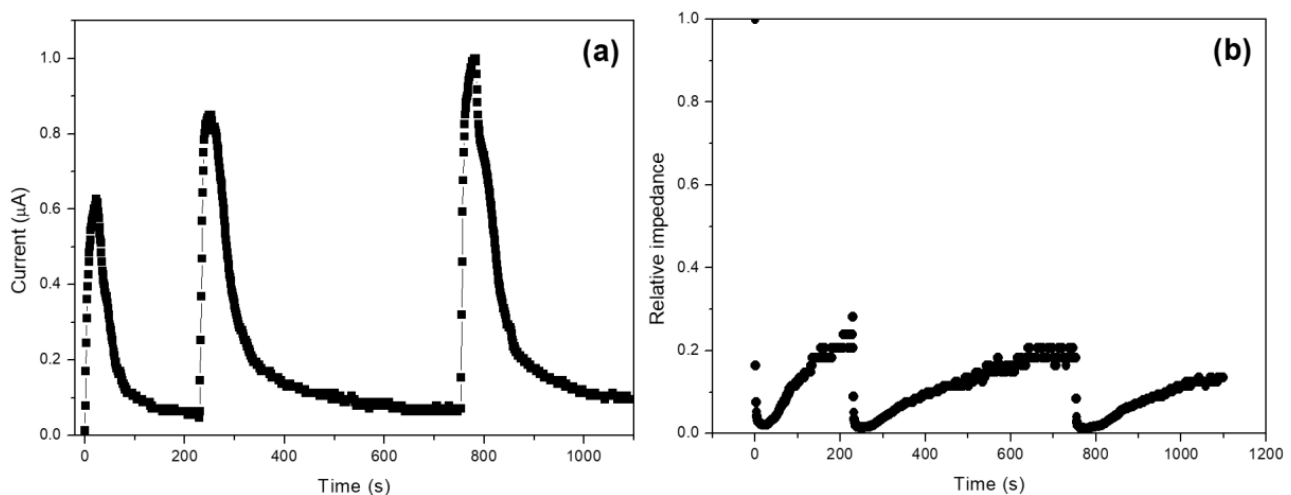


Figure 7. Exhalation signals displayed as time-resolved current intensity (a) and impedance (b).

The observed very fast response of the clinoptilolite-based sensor to the exhaled humidity is related to the special ionic transport mechanism that involves exclusively extra-framework cations located on the external surface of the zeolite slab. In fact, since the electrical contacts are located on the surface, only surface cations are subjected to the applied alternated electric field. During exhalation, these cations are directly exposed to the external humid environment, and, therefore, they readily interact with water molecular dipole by ion-cation electrostatic forces, thus leading to their hydration (solvation). The hydration process (involving one or more water molecules) significantly reduces the cation charge density, weakening, as a consequence, the Coulomb interaction between cations and the negative charge spread in the closed zeolite framework region (nucleophilic area). The consequent strong increase of cation mobility determines an increase in the current intensity moving on the slab surface, with a drop of the voltage between the silver electrodes. During inhalation, the low humidity content characterizing the environment close to the sensor surface determines a desorption of the water molecules from the cations (ion-dipole is a quite weak physical interaction) with restoration of the original very low surface conductivity of the zeolite slab. Such equilibrium between surface and environmental

water molecules allows the electrical monitoring of the moisture fluctuations in the space immediately close to the electrode surface.

4. Conclusions

A variety of ac square-wave voltage sources embedded into commercial entry-level digital multimeters (DMM) that are connected in parallel with a true-RMS voltmeter (voltage-drop method) have been tested to detect the signal coming from a simple clinoptilolite-based impedimetric water-vapor sensor. The most sensible response was observed with a square-wave voltage source of 14 μ W (maximum) embedded in the DT830D multimeter model. In particular, the water-vapor sensor was fabricated by cutting a piece of geomorphic natural clinoptilolite stone in form of small slab and painting two 1 mm-spaced rectangular electrodes on its surface. When the sensor was exposed to water vapor contained in the exhaled human breath, the slab surface impedance rapidly decreased, and this event was recorded as a voltage drop by the voltmeter data-logging system. Owing to the clinoptilolite surface hydrophobic nature, during the inhalation stage of the human breathing, water molecules rapidly desorbed from cations located on the external surface of the impedimetric sensor, thus determining a fast increase of its impedance value. The sensor showed a very prompt and completely reversible behavior at room temperature, thus allowing its technological exploitation as breath sensor. For example, this instrumental approach can be conveniently used for human-exhalation detection in apnea-syndrome monitoring. The principal physicochemical characteristics of the geomorphic clinoptilolite used for sensors fabrication were also determined by XRD and SEM/EDS.

Author Contributions: Conceptualization, G.C. and L.N.; Formal analysis, G.C.; Funding acquisition, G.C. Both authors have contributed equally to this research. All authors have read and agreed to the published version of the manuscript.

Funding: This research received no external funding.

Institutional Review Board Statement: Not applicable.

Informed Consent Statement: Not applicable.

Data Availability Statement: Not applicable.

Conflicts of Interest: The authors declare no conflict of interest.

References

1. Park, S.; Choi, K.S.; Lee, D.; Kim, D.; Lim, K.T.; Lee, K.-H.; Seonwoo, H.; Kim, J. Eggshell membrane: Review and impact on engineering. *Biosyst. Eng.* **2016**, *151*, 446–463. [[CrossRef](#)]
2. Sajid, M.; Aziz, S.; Kim, G.B.; Kim, S.W.; Jo, J.; Choi, K.H. Bio-compatible organic humidity sensor transferred to arbitrary surfaces fabricated using single-cell-thick onion membrane as both the substrate and sensing layer. *Sci. Rep.* **2016**, *6*, 30065. [[CrossRef](#)] [[PubMed](#)]
3. Su, B.; Gong, S.; Ma, Z.; Yap, L.W.; Cheng, W. Mimosa-Inspired Design of a Flexible Pressure Sensor with Touch Sensitivity. *Small* **2015**, *11*, 1886–1891. [[CrossRef](#)] [[PubMed](#)]
4. Potyrailo, R.A.; Ghiradella, H.; Vertiatchikh, A.; Dovidenko, K.; Cournoyer, J.R.; Olson, E. Morpho butterfly wing scales demonstrate highly selective vapour response. *Nat. Photon.* **2007**, *1*, 123–128. [[CrossRef](#)]
5. Potyrailo, R.A. Bio-inspired device offers new model for vapor sensing. *SPIE Newsroom* **2011**, *10*, 3568. [[CrossRef](#)]
6. Nassar, J.M.; Cordero, M.D.; Kutbee, A.T.; Karimi, M.A.; Torres Sevilla, G.A.; Hussain, A.M.; Shamim, A.; Hussain, M.M. Paper Skin Multisensory Platform for Simultaneous Environmental Monitoring. *Adv. Mater. Technol.* **2016**, *1*, 1600004. [[CrossRef](#)]
7. Vukusic, P.; Sambles, J. Photonic structures in biology. *Nature* **2003**, *424*, 852–855. [[CrossRef](#)]
8. Hovhannisyanyan, V.A.; Dong, C.-Y.; Lai, F.-J.; Chang, N.-S.; Chen, S.-J. Natural zeolite for adsorbing and release of functional materials. *J. Biomed. Opt.* **2018**, *23*, 91411. [[CrossRef](#)]
9. Ghobarkar, H.; Schäf, O.; Guth, U. Zeolites—From kitchen to space. *Prog. Solid St. Chem.* **1999**, *27*, 29–73. [[CrossRef](#)]
10. Sazama, P.; Jirglová, H.; Dedecek, J. Ag-ZSM-5 zeolite as high-temperature water-vapor sensor material. *Mater. Lett.* **2008**, *62*, 4239–4241. [[CrossRef](#)]
11. Schäf, O.; Wernert, V.; Ghobarkar, H.; Knauth, P. Microporous Stilbite single crystals for alcohol sensing. *J. Electroceramics* **2006**, *16*, 93–98. [[CrossRef](#)]

12. Kasperkowiak, M.; Strzemieska, B.; Voelkel, A. Characteristics of natural and synthetic molecular sieves and study of their interactions with fragrance compounds. *Physicochem. Probl. Miner. Process* **2016**, *52*, 789–802. [[CrossRef](#)]
13. Rhodes, C.J. Properties and applications of Zeolites. *Sci. Prog.* **2010**, *93*, 223–284. [[CrossRef](#)] [[PubMed](#)]
14. Tekin, R.; Erdogmus, H.; Bac, N. Assessment of zeolites as antimicrobial fragrance carriers. In *Antimicrobial Research: Novel Bioknowledge and Educational Programs*; Méndez-Villas, A., Ed.; Formatex Research Center: Badajoz, Spain, 2017. [[CrossRef](#)]
15. Simon, U.; Franke, M.E. *Ionic Conductivity of Zeolites: From Fundamentals to Applications, Host-Guest-Systems Based on Na-Noporous Crystals*; Laeri, F., Schüth, F., Simon, U., Wark, M., Eds.; Wiley-VCH Verlag GmbH & Co. KGaA: Weinheim, Germany, 2003; pp. 364–378.
16. Tabourier, P.; Carru, J.-C.; Wacrenier, J.-M. Dielectric and far-infrared investigation of cation movements in X-type zeolites. Study of their correlations. *J. Chem. Soc. Faraday Trans. 1 Phys. Chem. Condens. Phases* **1983**, *79*, 779–783. [[CrossRef](#)]
17. Freeman, D.C.; Stamires, D.N. Electrical conductivity of synthetic zeolites. *J. Chem. Phys.* **1961**, *35*, 799–806. [[CrossRef](#)]
18. Saly, V.; Kocalka, S. Dielectric response of natural clinoptilolite type zeolitic material containing silver iodide. *Chem. Pap.* **1996**, *50*, 328–333.
19. Qiu, P.; Huang, Y.; Secco, R.A.; Balog, P.S. Effect of multi-stage dehydration on electrical conductivity of zeolite A. *Solid State Ion.* **1999**, *118*, 281–285. [[CrossRef](#)]
20. Stamires, D.N. Effect of Adsorbed Phases on the Electrical Conductivity of Synthetic Crystalline Zeolites. *J. Chem. Phys.* **1962**, *36*, 3174–3181. [[CrossRef](#)]
21. Vučelić, D.; Juranic, N. The effect of sorption on the ionic conductivity of zeolites. *J. Inorg. Nucl. Chem.* **1976**, *38*, 2091–2095. [[CrossRef](#)]
22. Urbiztondo, M.; Pellejero, I.; Rodriguez, A.; Pina, M.; Santamaria, J. Zeolite-coated interdigital capacitors for humidity sensing. *Sens. Actuators B Chem.* **2011**, *157*, 450–459. [[CrossRef](#)]
23. Carotenuto, G.; Camerlingo, C. Kinetic investigation of water physisorption on natural clinoptilolite at room temperature. *Microporous Mesoporous Mater.* **2020**, *302*, 110238. [[CrossRef](#)]
24. Lin, C.C.H.; Dambrowitz, K.A.; Kuznicki, S.M. Evolving applications of zeolite molecular sieves. *Can. J. Chem. Eng.* **2011**, *90*, 207–216. [[CrossRef](#)]
25. Carotenuto, G. Electrical Investigation of the Mechanism of Water Adsorption/Desorption by Natural Clinoptilolite Desiccant Used in Food Preservation. *Mater. Proc.* **2020**, *2*, 15. [[CrossRef](#)]
26. Kowalczyk, P.; Sprynskyy, M.; Terzyk, A.P.; Lebedynets, M.; Namieśnik, J.; Buszewski, B. Porous structure of natural and modified clinoptilolites. *J. Colloid Interface Sci.* **2006**, *297*, 77–85. [[CrossRef](#)] [[PubMed](#)]
27. Duan, Z.; Jiang, Y.; Tai, H. Recent advances in humidity sensors for human body related humidity detection. *J. Mater. Chem. C* **2021**, *9*, 14963–14980. [[CrossRef](#)]
28. Duan, Z.; Zhao, Q.; Wang, S.; Huang, Q.; Yuan, Z.; Zhang, Y.; Jiang, Y. Halloysite nanotubes: Natural, environmental-friendly and low-cost nanomaterials for high-performance humidity sensor. *Sens. Actuators B Chem.* **2020**, *317*, 128204. [[CrossRef](#)]
29. Duan, Z.; Jiang, Y.; Zhao, Q.; Wang, S.; Yuan, Z.; Zhang, Y.; Liu, B.; Tai, H. Facile and low-cost fabrication of a humidity sensor using naturally available sepiolite nanofibers. *Nanotechnology* **2020**, *31*, 355501. [[CrossRef](#)] [[PubMed](#)]
30. Duan, Z.; Zhao, Q.; Wang, S.; Yuan, Z.; Zhang, Y.; Li, X.; Wu, Y.; Jiang, Y.; Tai, H. Novel application of attapulgite on high performance and low-cost humidity sensors. *Sens. Actuators B Chem.* **2020**, *305*, 127534. [[CrossRef](#)]
31. Serban, B.-C.; Cobianu, C.; Buiu, O.; Bumbac, M.; Dumbravescu, N.; Avramescu, V.; Nicolescu, C.M.; Brezeanu, M.; Radulescu, C.; Cracium, G.; et al. Quaternary holey carbon nanohorns/SnO₂/ZnO/PVP nano-hybrid as sensing element for resistive-type humid sensor. *Coatings* **2021**, *11*, 1307. [[CrossRef](#)]
32. Zhang, Y.; Wu, Y.; Duan, Z.; Liu, B.; Zhao, Q.; Yuan, Z.; Li, S.; Liang, J.; Jiang, Y.; Tai, H. High performance humidity sensor based on 3D mesoporous Co₃O₄ hollow polyhedron for multifunctional applications. *Appl. Surf. Sci.* **2022**, *585*, 152698. [[CrossRef](#)]
33. Matko, V.; Milanovič, M. Detection principles of temperature compensated oscillators with reactance influence on piezoelectric resonator. *Sensors* **2020**, *20*, 802. [[CrossRef](#)] [[PubMed](#)]
34. Mogera, U.; Sagade, A.A.; George, S.J.; Kulkarni, G.U. Ultrafast response humidity sensor using supramolecular nanofiber and its application in monitoring breath humidity and flow. *Sci. Rep.* **2014**, *4*, 4103. [[CrossRef](#)] [[PubMed](#)]
35. Liao, F.; Zhu, Z.; Yan, Z.; Yao, G.; Huang, Z.; Gao, M.; Pan, T.; Zhang, Y.; Li, Q.; Feng, X.; et al. Ultrafast response flexible breath sensor based on vanadium dioxide. *J. Breath Res.* **2017**, *11*, 36002. [[CrossRef](#)] [[PubMed](#)]
36. Yang, Y.; Gao, W. Wearable and flexible electronics for continuous molecular monitoring. *Chem. Soc. Rev.* **2019**, *48*, 1465–1491. [[CrossRef](#)] [[PubMed](#)]